

A Novel Strain Sensor Based on 3D Printing Technology and 3D Antenna Design

Taoran Le¹, Bo Song², Qi Liu^{3,1}, Ryan A. Bahr¹, Stefano Moscato¹, Ching-Ping Wong², and Manos. M. Tentzeris¹

¹The School of Electrical and Computer Engineering

²The School of Material Science Engineering

Georgia Institute of Technology

Atlanta, U.S.A.

³ Center for Optical and Electromagnetic Research

Zhejiang University

Hangzhou, China

taoran.le@ece.gatech.edu

Abstract

The additive manufacturing technique of 3D printing has become increasingly popular for time-consuming and complex designs. Due to the special mechanical properties of commercial NinjaFlex filament [1] and in-house-made electrically conductive adhesives (ECAs) [2], there is great potential for the 3D printed RF applications, such as strain sensors and flexible, wearable RF devices. This paper presents the flexible 3D printed strain sensor, as a 3D dipole antenna of ECA stretchable conductor on 3D printed NinjaFlex filament.

Index Terms — *3D printing, materiel characterization, stretchable, 3D antenna, NinjaFlex, flexible electronics, RF.*

I. Introduction

3D printer has been around 30 years. 3D printing is the technology of building physical objects up layer by layer, based on detailed digital blueprint [3]. Even 3D printing has been used in some industry for a while, but open sourced softwares, the lower-cost of 3D printers and more and more 3D printing materials really bring 3D printing technology to the mainstream. The advantages of the 3D printing technology include time-saving and the capability to fabricate the complex structure with multiple materials which are out of the capability of the standard fabrication methods. It's very clear that more and more 3D printed applications will show up in the near future.

NinjaFlex filament was introduced by Fenner Drives, Inc. in 2014 as one of the newest 3D printing materials in the market [4]. It is one type of thermoplastic elastomers (TPEs) which are combinations of a thermoplastic and a rubber [5], potentially enabling 3D printing to be applied to numerous new areas, such as wearable RF electronics and antennas, due to its extremely high flexibility and stretchability. Shortly after its release, NinjaFlex was utilized on a wide variety of projects [6,7]. This paper presents the electrical characterization of the NinjaFlex filament (color: Snow) at UHF band and a wireless strain sensor based on 3D printed NinjaFlex and stretchable conductor ECAs.

Meanwhile, stretchable electronics are gaining popularity in the highly demanding field of wearable devices. A commonly used approach is to maintain the conventional circuit layout but embed stretchable or flowable conductive materials, such as conductive polymers [8] conductive polymer composites [9], and liquid metal alloys [10] as stretchable conductive lines. In this paper we chose to use stretchable ECAs as the

stretchable conductive material. The ECAs feature a higher conductivity ($1.51 \times 10^6 \text{ Sm}^{-1}$) than most previously reported stretchable conductors [8,9]. More importantly, the conductivity of ECAs is as high as $1.11 \times 10^5 \text{ Sm}^{-1}$ at a strain of 240% and remains almost invariant over 500 cycles of stretching at 100% applied strain [2]. These ECAs are highly suitable for building stretchable RF devices.

In this paper, a 3D dipole antenna was designed in commercial full wave simulator ANSYS HFSS as a preliminary proof-of-concept prototype. The substrate is 3D printed NinjaFlex. The antenna is made of in-house-made ECAs.

The 3D printing of NinjaFlex filament and the RF characterization of it are present in section II. The ECAs strain test results are included in section III. The 3D antenna design is detailed in section VI. At last, section V is about the strain test results of this 3D printed strain sensor.

II. 3D printing NinjaFlex and NinjaFlex RF characterization

A. 3D printing NinjaFlex

Most commercial low-cost 3D printers today are using fused deposition modeling (FDM), of which the patent was first filled back to 1989 by S. Scott Crump [11]. This technology feeds a plastic filament into a heated extruder and then precisely lays down the material [3]. A variety of adjustable options of this technique affect the printing quality. Important properties include layer height, amount of top and bottom solid layers, amount of perimeter walls, solid/infill patterns, and infill densities.

A layer height of 100 microns is considered standard and is achievable for most 3D printers in the market today, such as the Stratasys Dimension 1200es and the Printbot Simple Metal [12,13]. The amount of top and bottom layers both affects the mechanical strength of those sides; if there are not enough layers, the top layer may become porous. An increase in the amount of perimeter walls increases the strength of the print, but one wall suffices to create a non-porous surface. Infill patterns are shown in Fig. 1. During testing, a Hilbert curve pattern is preferable for solid layers to create a non-porous bottom and top layer. As many printers by default print rectilinear, the rectilinear pattern was chosen for fabrication repeatability among different printer models [12]. The infill density can be varied, and the material is typically characterized for densities of 40%, 70%, and 100%, which can lead to varying mechanical properties.

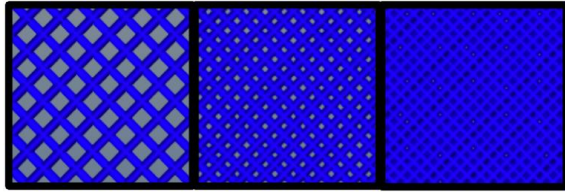


Fig.1. Variety of infill Rectilinear patterns available to print in slic3r. Left to Right: 40%, 70%,100%.

The 3D antenna presented in this paper was fabricated on a 100% infill density cube shell. All samples tested are made on the Hyrel [14] System 30 3D printer, as shown in Fig. 2. This hardware uses a modified version of the Repetier controller software called Repetrel, which still uses the common slicing CAD software slic3r [15,16].

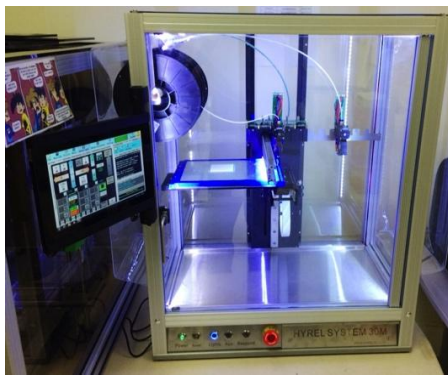


Fig.2. Hyrel System 30 3D printer

B. NinjaFlex RF characterization

The most important characteristics of a new material are the dielectric permittivity and the loss tangent for a microwave designer. Due to the lack of information of NinjaFlex's electromagnetic properties, a microstrip-fed ring resonator was chosen for the material characterization due to the size and accuracy requirements over the UHF band of interest [17].

The design of the ring-resonator is aided by the ANSYS HFSS. Two microstrip feeding lines are adopted to excite the ring and to collect the transmitted power. These feeding lines are separated by the resonator through 0.8 mm gaps. The width is set to achieve a characteristic impedance as close as possible to 50 Ohms by assuming a dielectric permittivity close to 3 and a substrate thickness of 1.27 mm. The gap is set intentionally large in order to more accurately get the loaded and unloaded quality factors of the resonator in case the transmitted power is very low and noisy measurements are expected. Moreover, this distance is also chosen to relax the constraints due to the process variations.

The design of the central part of this component, the ring, concerns mainly two dimensions: the radius and the width of the strip. The first one is set to achieve a resonant frequency as close as possible to 2.4 GHz. Starting from this point, the width of the ring strip has to be chosen in order to avoid higher modes [18] and to take into account the constraints of

the manufacturing technique. As the ratio of the width and the summation of inner and outer radius has to be lower than 0.05, the chosen width is the maximum one that satisfies this relationship. The final design of the resonator is shown in Fig. 3.

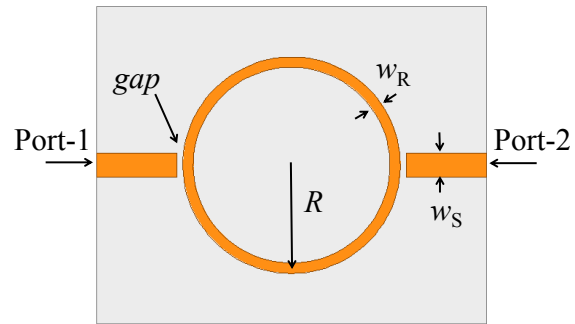


Fig. 3. Design of the ring resonator. The distance between Port-1 and Port-2 is 48.9 mm while the overall width of the substrate is 40 mm. $w_S=3$ mm $gap=0.8$ mm $R=13$ mm $w_R=1.3$ mm

The ring structure is manufactured on three different substrates made of NinjaFlex of 40%, 70% and 100% densities. As the material has never been adopted for any electronics application, a proper manufacturing technique has been chosen. Since chemical etching involves acids the risk in damaging NinjaFlex through non-mechanical methods is very high. Inkjet printing is a possibility for characterization. The main issue concerns the porosity that a 3D printed material can exhibit and this deeply affects the layers of conductive ink. The last option is to employ a high precision milling machine, widely adopted for in-lab PCB realization. A 0.025 mm thick copper foil is stacked on the top of the substrate through a thin layer of epoxy glue. The Gorilla Glue epoxy solidifies allowing the milling machine to mill with additional precision [19]. The electromagnetic characterization hereby proposed exploits not only the dielectric substrate but also considers the thin film of glue that is required to manufacture copper clad NinjaFlex. The bottom is fully grounded through being covered with copper tape. The measurement setup involves a R&S®ZVA8 vector network analyzer (VNA). The input and output feeding lines are connected to the VNA thanks to standard SMA-to-microstrip connectors fastened to the circuit with conductive epoxy glue. The ring resonator under test is shown in Fig. 4.

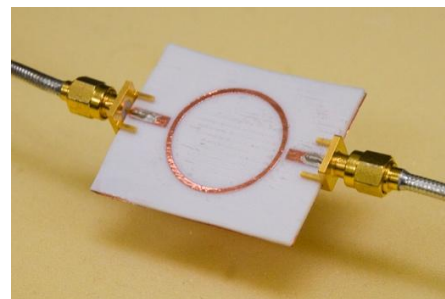


Fig. 4. The ring resonator realized on the NinjaFlex substrate.

Fig. 5 shows the frequency peaks for the three different densities. As expected, the higher infill densities lower the resonant frequency. This phenomenon is due to the high percentage of air in the substrate for low infill sample, that lowers the permittivity. Starting from these measurements the dielectric permittivity can be retrieved for each sample [17].

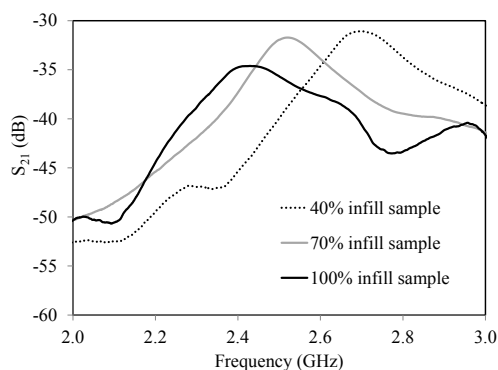


Fig. 5. Measurements of the transmission parameter of the three different ring resonators. The frequency shift due to different infill percentages can be noticed.

Fig. 6 shows the value of ϵ_r versus the infill percentage as well as the calculated loss tangent for the same substrates. The results show high losses compared to standard microwave substrates and as expected, the higher value of loss tangent is related to the sample with 100% of infill.

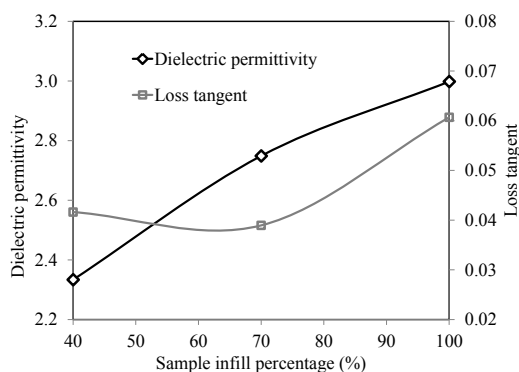


Fig. 6. Dielectric permittivity and loss tangent versus the infill percentage of the NinjaFlex sample.

III. The stretchable high conductive ECAs

A. The conductivity of ECAs

High conductivity is one of the most critical requirements for the ECAs to be used in stretchable antennae, because it will affect the conduction loss and thus the radiation efficiency.

The long-chain hydride-terminated polydimethyl siloxane (H-PDMS) is used as the curing agent of the ECA. Commercial silver flakes are usually covered with a thin layer of lubricant, whose component is generally long chain fatty acid. The carboxylic group of the fatty acid can coordinates with the silver surface and form a silver carboxylate salt

complex, while the hydrocarbon chain can facilitate the dispersion of silver flakes and prevent oxidation [20]. However, these lubricants are insulating by nature, posing a significant energy barrier to electron conduction between neighboring silver flakes. Therefore, reducing agents were added to ECAs to chemically reduce the lubricant to nano/submicron-sized silver particles and these in situ formed nano/submicron-sized particles may then facilitate the sintering of the silver flakes during curing [21]. As a result, the high molecular weight of long-chain H-PDMS not only provides a high elasticity due to the low cross-linking density of the formed silicone matrix, but also enhance the electrical conductivity via the generation and sintering of silver nanoparticles [22].

The second modification made to the filler particles is the iodination of the silver flakes before mixing with the silicone matrix. It was found that nonstoichiometric Ag/AgI nanoislands sparsely form on the silver flake surface after immersion of the flakes in dilute iodine/ethanol solution. The continuous decomposition and formation of AgI initiate the reconstruction of the silver flakes surface [2]. The exposure of fresh silver at the flake surface further facilitates the sintering between silver flakes during curing. The combination of these two surface modification methods can form a strong electron conduction network and reach an initial conductivity of of $1.51 \times 10^6 \text{ Sm}^{-1}$ filled with 80 wt.% silver flakes, which is comparable with conventional epoxy-based ECAs and in the same order of magnitude with many metals [23].

B. The conductivity of the ECAs under strain

The largest challenge for stretchable electronics, especially RF devices, is that the conductivity has a significant drop under a certain mechanical strain.

The antenna traces have been 3D printed by the NinjaFlex filament. The in-house ECA was filled into these traces to fabricate the 3D antenna then was cured at 150C for one hour. This curing temperature ensures a more complete sintering of the silver nanoparticles, thus enhancing the overall electrical conductivity.

For the conductivity measurement during stretching, a strip of silo-ECA is printed on silicone substrate and cut into a dumbbell shape. The specimen is then mounted on a tensile tester (Instron Microtester 5548). Real-time electrical resistance change is measured by a typical four-wire method with all the wires “soldered” to the silo-ECA stripe with additional silo-ECA and the applied strain is simultaneously recorded by the tensile tester. The conductivity of the silo-ECA drops to $5.03 \times 10^3 \text{ S cm}^{-1}$ after embedding in the substrate, yet it is still higher than most previously reported stretchable conductors. Fig.7 shows the conductivity change as a function of the applied tensile strain of the silo-ECA as compared with previously reported stretchable conductors. A general trend is visible; the metal-filled conductive composites [24-26] have significantly higher conductivity than carbon-filled conductive composites [27-31], while some CNT-based composites can maintain a high conductivity at a larger elongation due to their high-aspect

ratio [30]. The conductivity of the ECA is two orders of magnitude higher than that of conventional silver/PDMS composites [25] due to the surface treatments mentioned above, and is comparable with gold nanoparticle/polyurethane composites [26]. More importantly, silo-ECA has better elasticity than previously reported metal/polymer composites and can maintain a high conductivity at large deformations. For example, even at a strain of 240%, the conductivity is still as high as $1.11 \times 10^3 \text{ S cm}^{-1}$, indicating that the external stress only leads to sliding between overlapping flakes and does not change the tunneling distance significantly. In addition, the conductivity change is within 25% after 1000 cycles of stretching at 50% applied strain, as shown in Fig.8..

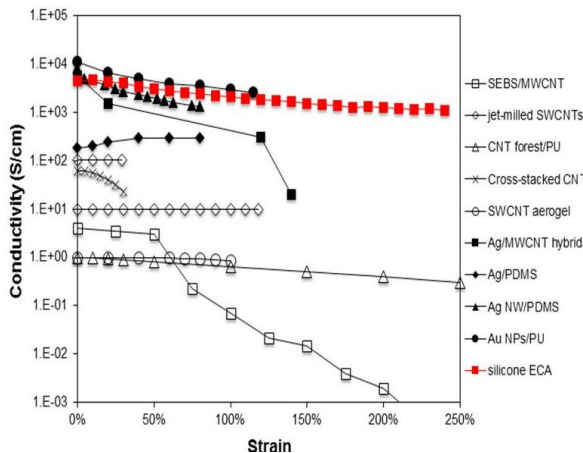


Fig.7. Conductivity change of the in-house made ECSs as a function of tensile strain, as compared with the values from previous studies.

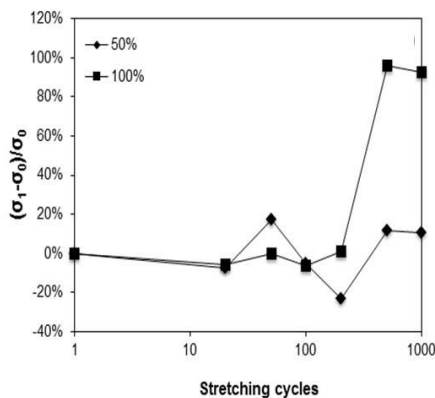


Fig.8. The conductivity of ECAs after cycling at 50% strain and 100% strain

VI. 3D printed strain sensor prototype

A. 3D antenna design

The geometry of the proposed dipole antenna is depicted in Fig. 9. The substrate is a 30mm×30mm×30mm hollow cube made of NinjaFlex (relative permittivity 2.98 and loss tangent 0.06 @ 2.4 GHz). The dipole antenna with two perpendicular arms is made of ECAs. As shown in the Fig.9 (a), the dipole is placed on the top surface of the cube and bend toward two other surfaces on the side. The feed part of the dipole is right in the center of the top surface. The two

arms extend to the edge of the top surface, then bend along two other vertical surfaces. This 3D structure makes it simple to quantitative analyze the antenna topology change caused by strain.

The cube has a hollow cube in the middle. The reason for this structure design is to increase the quantity of printing NinjaFlex and easy to stretch the part of the dipole antenna on the front surface in Fig.9. The added strain directions are shown in Fig.9 (b).

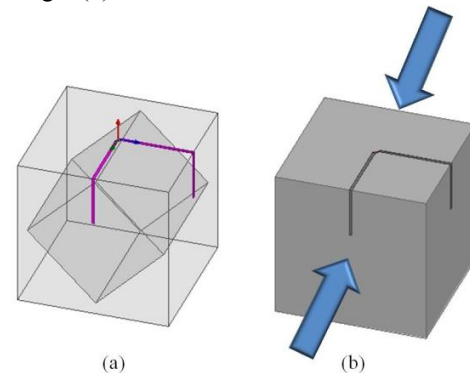


Fig.9. (a) 3D antenna on a hollow cube; (b) To add strain on the front and the back surfaces of the cube.

B. The 3D printed strain sensor prototype

The cube with antenna traces was first 3D printed by Hyrel System 30 3D printer using NinjaFlex filament. Then the antenna traces were filled by the ECAs based on the design in ANSYS HFSS. Between the two antenna trace, a impedance matched balun was added to connect with a SMA connector for insertion loss test, as shown in Fig. 10.

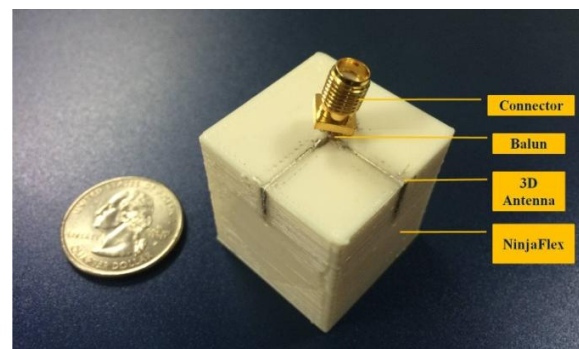


Fig.10. The ready-to-test 3D printed strain sensor

V. Strain experiments and results

The strain experiment is to add strain on the front and the back sides of the cube (Fig.9. (b)) and to observe the frequency shift of the center frequency of the antenna. There were two different levels of strain added on the cube during the experiment. The measurement results are presented in the solid lines in the Fig.11. 30MHz and 50MHz of the center frequency shifts were observed by the strain1 and strain2.

Due to the cube 3D structure, the most significant length change of the antenna is the part of the antenna on the front side of the cube. After adding strain on it, this part of the antenna was stretched by stretched NinjaFlex. So the center frequency of the antenna was decreasing as expected.

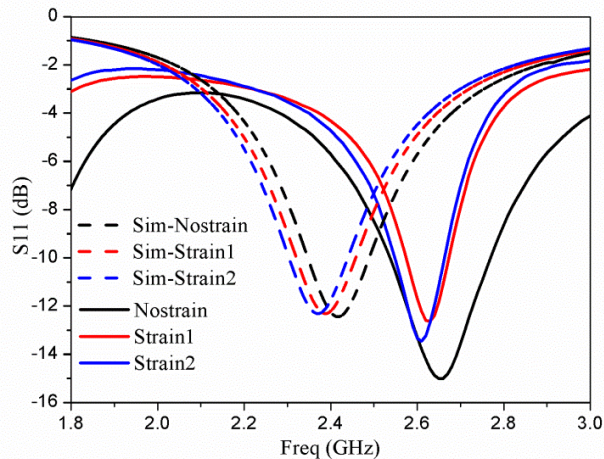


Fig.11. The measurement results and the simulation results of the strain test on the 3D printed strain sensor

In HFSS, 0.6mm and 1mm were added on the antenna part of the front side of the cube, the same trend of the center frequency shift was observed, as shown in the dash lines in the Fig.11. 30MHz and 50MHz of the center frequency shifts were caused by the 0.6mm and 1mm added on the 10mm part of the antenna on the front side of the cube.

We noticed that the center frequency of the antenna has 200MHz shift. It might be caused by filling ECAs into traces process. In the future, we plan to 3D printing ECAs and NinjaFlex at the same time by two nozzles on the Hyrel System.

VI. Conclusions

The first ever 3D printed flexible RF strain sensor system was presented in this paper. The common 3D printing material - NinjaFlex was RF characterized and a 3D antenna was designed and fabricated by NinjaFlex and stretchable ECAs as well. It brings a huge potential for future 3D printed RF applications, such as wearable RF circuits and 3D flexible sensors.

Acknowledgments

The authors would like to thank DTRA for their support of the research.

References

1. <http://www.ninjaxflex3d.com/>
2. Li, Zhuo, Taoran Le, Zhenkun Wu, Yagang Yao, Liyi Li, Manos Tentzeris, Kyoung-Sik Moon, and C. P. Wong. "Rational Design of a Printable, Highly Conductive Silicone-based Electrically Conductive Adhesive for Stretchable Radio-Frequency Antennas." *Advanced Functional Materials* 25, no. 3 (2015): 464-470.
3. Make: Volume 41, the Ultimate Guide to 3D Printing 2014
4. <http://www.ninjaxflex3d.com/>
5. Hovath, J, *Mastering 3d Printing*. New York: Apress, 2014. pp. 85.
6. "Quack-Quack the duck gets his 3D printed leg brace and the chance to walk again," 3Ders, August 13, 2014 [Online] Available: <http://3ders.org>

7. "3D Technology Kicks at the World Cup," *Product Design & Development*, June 12, 2014. [Online]. Available: <http://www.pddnet.com/news/2014/06/3d-technology-kicks-world-cup>
8. Verma, Akhilesh, Bo Weng, Roderick Shepherd, Christophe Fumeaux, Van-Tan Truong, Gordon G. Wallace, and Bevan D. Bates. "6 GHz microstrip patch antennas with PEDOT and polypyrrole conducting polymers." In *Electromagnetics in Advanced Applications (ICEAA), 2010 International Conference on*, pp. 329-332. IEEE, 2010.
9. Agar, J., J. Durden, D. Staiculescu, R. Zhang, E. Gebara, and C. P. Wong. "Electrically conductive silicone nanocomposites for stretchable RF devices." In *Microwave Symposium Digest (MTT), 2011 IEEE MTT-S International*, pp. 1-4. IEEE, 2011.
10. Kubo, Masahiro, Xiaofeng Li, Choongik Kim, Michinao Hashimoto, Benjamin J. Wiley, Donhee Ham, and George M. Whitesides. "Stretchable microfluidic radiofrequency antennas." *Advanced materials* 22, no. 25 (2010): 2749-2752.
11. Crump, S. Scott. "Apparatus and method for creating three-dimensional objects." U.S. Patent 5,121,329, issued June 9, 1992.
12. <http://www.stratasys.com/3d-printers/design-series/dimension-1200es>
13. <http://printrbot.com/shop/assembled-simple-metal/>
14. <http://www.hyrel3d.com/>
15. <http://www.repetier.com/>
16. <http://slic3r.org/>
17. Yang, Li, Amin Rida, Rushi Vyas, and Manos M. Tentzeris. "RFID tag and RF structures on a paper substrate using inkjet-printing technology." *Microwave Theory and Techniques, IEEE Transactions on* 55, no. 12 (2007): 2894-2901.
18. L.-F. Chen, C.-K. Ong, C.-P. Neo, V.-V. Varadan and V.-K. Varadan, *Microwave Electronics Measurement and Materials Characterization*, John Wiley & Sons, 2004.
19. <http://www.gorillaglu.com/gorilla-epoxy>
20. Lu, Daoqiang, Quinn K. Tong, and C. P. Wong. "A study of lubricants on silver flakes for microelectronics conductive adhesives." *Components and Packaging Technologies, IEEE Transactions on* 22, no. 3 (1999): 365-371
21. Zhang, Rongwei, Kyoung-sik Moon, Wei Lin, Josh C. Agar, and Ching-Ping Wong. "A simple, low-cost approach to prepare flexible highly conductive polymer composites by in situ reduction of silver carboxylate for flexible electronic applications." *Composites Science and Technology* 71, no. 4 (2011): 528-534.
22. Li, Zhuo, Kristen Hansen, Yagang Yao, Yanqing Ma, Kyoung-sik Moon, and C. P. Wong. "The conduction development mechanism of silicone-based electrically conductive adhesives." *Journal of Materials Chemistry C* 1, no. 28 (2013): 4368-4374.
23. Zhang, Rongwei, Wei Lin, Kyoung-sik Moon, and C. P. Wong. "Fast preparation of printable highly conductive polymer nanocomposites by thermal decomposition of silver carboxylate and sintering of silver nanoparticles."

- ACS applied materials & interfaces 2, no. 9 (2010): 2637-2645.
24. Chun, Kyoung-Yong, Youngseok Oh, Jonghyun Rho, Jong-Hyun Ahn, Young-Jin Kim, Hyouk Ryeol Choi, and Seunghyun Baik. "Highly conductive, printable and stretchable composite films of carbon nanotubes and silver." *Nature nanotechnology* 5, no. 12 (2010): 853-857.
 25. Niu, X. Z., S. L. Peng, L. Y. Liu, W. J. Wen, and Ping Sheng. "Characterizing and patterning of PDMS-based conducting composites." *Advanced Materials* 19, no. 18 (2007): 2682-2686.
 26. Kim, Yoonseob, Jian Zhu, Bongjun Yeom, Matthew Di Prima, Xianli Su, Jin-Gyu Kim, Seung Jo Yoo, Ctirad Uher, and Nicholas A. Kotov. "Stretchable nanoparticle conductors with self-organized conductive pathways." *Nature* 500, no. 7460 (2013): 59-63.
 27. Sekitani, Tsuyoshi, Yoshiaki Noguchi, Kenji Hata, Takanori Fukushima, Takuzo Aida, and Takao Someya. "A rubberlike stretchable active matrix using elastic conductors." *Science* 321, no. 5895 (2008): 1468-1472.
 28. Sekitani, Tsuyoshi, Hiroyoshi Nakajima, Hiroki Maeda, Takanori Fukushima, Takuzo Aida, Kenji Hata, and Takao Someya. "Stretchable active-matrix organic light-emitting diode display using printable elastic conductors." *Nature materials* 8, no. 6 (2009): 494-499.
 29. Li, Yongjin, and Hiroshi Shimizu. "Toward a stretchable, elastic, and electrically conductive nanocomposite: morphology and properties of poly [styrene-*b*-(ethylene-co-butylene)-*b*-styrene]/multiwalled carbon nanotube composites fabricated by high-shear processing." *Macromolecules* 42, no. 7 (2009): 2587-2593.
 30. Shin, Min Kyoon, Jiyoung Oh, Marcio Lima, Mikhail E. Kozlov, Seon Jeong Kim, and Ray H. Baughman. "Elastomeric conductive composites based on carbon nanotube forests." *Advanced Materials* 22, no. 24 (2010): 2663-2667.
 31. Kim, Kyu Hun, Mert Vural, and Mohammad F. Islam. "Single-Walled Carbon Nanotube Aerogel-Based Elastic Conductors." *Advanced materials* 23, no. 25 (2011): 2865-2869.